TransCom 3: Annual Mean CO2 Flux Estimates from Atmospheric Inversions (Level 1)

Abstract

Information about regional carbon sources and sinks can be derived from variations in observed atmospheric CO_2 concentrations via inverse modeling with atmospheric tracer transport models. A consensus has not yet been reached regarding the size and distribution of regional carbon fluxes obtained using this approach, partly owing to the use of several different atmospheric transport models.

Under TransCom 3, surface-atmosphere CO_2 fluxes were estimated from an intercomparison of 16 different atmospheric tracer transport models and model variants in order to assess the contribution of uncertainties in transport to the uncertainties in flux estimates for annual mean, seasonal cycle, and interannual inversions (referred to as Level 1, 2, and 3 experiments, respectively). The TransCom 3 experiments also contribute to the understanding of other sensitivities in the inversion process (e.g. inversion set-up, observational data choices) since more reliable results are expected by examining the sensitivity with a range of transport models than with just one or two models.

This data set provides the model output and inversion results for the TransCom 3, Level I annual mean inversion experiments. Annual mean CO_2 concentration data (GLOBALVIEW-CO_2, 2000) were used to estimate CO_2 sources. The annual average fluxes were estimated for the 1992-1996 period using each of the 16 transport models and a common inversion set-up (Gurney et al., 2002). Methodological choices for this control inversion were selected on the basis of knowledge gained from a wide range of sensitivity tests (Law et al., 2003). Gurney et al. (2003) present results from the control inversion for individual models as well as results from a number of sensitivity tests related to the specification of prior flux information. Law et al. (2003) present sensitivity tests related to CO_2 data issues including network choice, time period, data selection, and data uncertainty. Performing the inversion with multiple transport models gives mean estimated fluxes that are relatively insensitive to reasonable variations in the set-up -- and estimated uncertainties that represent a more complete estimate of the true uncertainty.

The results from TransCom 3 Level 2 (seasonal) and Level 3 (interannual) inversion experiments will be archived by ORNL DAAC at a later date.

Background Information

Investigators:

Kevin R. Gurney (kevin.gurney@asu.edu)
Purdue University

A. Scott Denning (denning@atmos.colostate.edu)
Colorado State University

Contributors:

Rachel M. Law, Commonwealth Scientific and Industrial Research Organization (CSIRO)
Peter J. Rayner, CSIRO
Robert Baker, NCAR
Philippe Bousquet, Laboratoire des Sciences du Climat et de l'Environment (LSCE)
Lori Bruhwiler, NOAA Climate Monitoring and Diagnostic Laboratory (CMDL)
Yu-Han Chen, Dept. Earth, Atmospheric and Planetary Science, MIT
Philippe Ciais, LSCE
Songmiao Fan, AOS Program, Princeton University
Inez Y. Fung, Center for Atmospheric Sciences, University of California, Berkeley
Manuel Gloor, Max-Planck Institute fur Biogeochemie, Jena
Martin Heimann, Max-Planck, Jena
Kaz Higuchi, Meteorological Service of Canada, Environment Canada
Jasmin John, Center for Atmospheric Sciences, UC, Berkeley
Eva Kowalczyk, CSIRO
Tasashi Maki, QA Section, Atmospheric Envir. Div., Observations Dept, Japan Met. Agency
Shamil Maksyutov, Inst. for Global Change Res., Frontier Res. Sys. for Global Change, Japan
Philippe Peylin, LSCE
Michael Prather, Earth System Science, University of California, Irvine
Bernard C. Pak, Earth System Science, UC, Irvine
Jorge Sarmiento, AOS Program, Princeton University
Shoichi Taguchi, National Institute of Advanced Industrial Science and Technology, Japan
Taro Takahashi, Lamont-Doherty Earth Observatory of Columbia University
Chiu-Wai Yuen, Meteorological Service of Canada, Environment Canada

Project:

International Geosphere-Biosphere Programme (IGBP)
Global Analysis, Interpretation, and Modeling Project (GAIM)

Web Site: http://transcom.project.asu.edu/index.php

Data Set Title: TransCom 3: Annual Mean CO2 Flux Estimates from Atmospheric Inversions (Level 1)

Site: Global (Gridded)

Westernmost Longitude: -180 W
Easternmost Longitude: 180 E
Northernmost Latitude: 90 N
Southernmost Latitude: -90 S

Data Set Citation:

Gurney, K. R. and A. S. Denning. 2006. TransCom 3: Annual Mean CO2 Flux Estimates from Atmospheric Inversions (Level 1). Data set. Available on-line [http://daac.ornl.gov/] from Oak Ridge National Laboratory Distributed Active Archive Center, Oak Ridge, Tennessee, U.S.A. doi: 10.3334/ORNLDAAC/895.

Background on TransCom Experiments

The Atmospheric Tracer Transport Model Intercomparison Project (TransCom) was created to quantify and diagnose the uncertainty in inversion calculations of the global carbon budget that result from errors in simulated atmospheric transport, the choice of measured atmospheric carbon dioxide data used, and the inversion methodology employed. TransCom was conceived at the Fourth International CO_2 Conference in Carqueiranne, France in 1993. The project is part of a larger International Geosphere-Biosphere Programme (IGBP), Global Analysis, Interpretation, and Modeling (GAIM) research program which aims to develop coupled ecosystem-atmosphere models that describe time evolution of trace gases with changing climate and changes in anthropogenic forcing.

Initially coordinated by Peter Rayner at the Commonwealth Scientific and Industrial Research Organization (CSIRO), TransCom is now being coordinated by Scott Denning at the Department of Atmospheric Sciences, Colorado State University and Kevin Gurney formerly at the Department of Atmospheric Sciences, Colorado State University and now at Department of Earth and Atmospheric Sciences & Department of Agronomy, Purdue University. Three distinct phases of the TransCom have now been completed. Investigators are currently in the process of planning and coordinating a new future for the TransCom community.

TransCom 1

The first phase of TransCom, which involved about a dozen modeling groups from around the world, examined the atmospheric concentration response to surface emissions of fossil fuel CO_2 and the activity of terrestrial ecosystems. These experiments were designed to address two salient features of atmospheric CO_2: (1) the annual mean north-south (meridional) gradient arising from fossil fuel emissions; and (2) the seasonal cycle arising from the seasonal exchange of CO_2 between the atmosphere and terrestrial ecosystems, with a net zero flux at each grid point but with strong uptake during the growing season balanced by release by decomposition.

Results of this initial intercomparison were reported by Rayner and Law (1995) and Law et al. (1996). With a few exceptions, there was good agreement among the models with regard to the annual mean meridional distribution of the "fossil fuel" tracer at the surface. A few models simulated extremely strong interhemispheric gradients of fossil-fuel at the surface, and these models also simulated very low concentrations aloft over the emissions region. This suggests that the high surface mixing ratios simulated by these models resulted from vertical trapping of tracer in the emissions region, rather than from weak interhemispheric transport.

There was qualitative agreement for the seasonal variations of CO_2 in the biosphere experiment, although this agreement diminishes over continental regions which lack observational constraints. The annual mean meridional response of the models to seasonal biotic forcing can be classified into two groups. Models which represent turbulent mixing in the planetary boundary layer (PBL) simulate a pole-to-pole gradient in surface CO_2 that is roughly half as strong as that obtained in the fossil fuel experiment. The other models simulate a very weak meridional structure in these runs.

TransCom 2

The results of the Phase 1 experiments showed a some differences among the participating models, but observations of CO_2 arising purely from fossil fuel emissions or seasonal vegetation do not exist. Evaluation of the realism of the various model simulations is therefore impossible. In 1996, the participants agreed to perform additional experiments to “calibrate” the results of TransCom 1, and in addition, seek to understand the mechanisms by which the models diverged in their results (Denning et al., 1999). With an extremely long atmospheric lifetime, a relatively well-known source, and a twenty year legacy of observations around the planet, sulfur hexafluoride (SF_6) is an ideal trace gas for transport calibration purposes.

While most of the models were reasonably successful at reproducing the "background" observations of SF_6, some underestimated marine boundary layer values due to excessive vertical convective transport. Many of the models were less successful at continental locations near sources, where most models significantly overestimated SF_6. The “more convective” models matched the observations better at these continental sites than did the “less convective” ones. These results further emphasize the TransCom 1 findings that strong meridional gradients in simulated fossil fuel CO_2 at the surface were systematically associated with weak meridional gradients in the upper troposphere, and vice versa.

Although there were distinct differences in the intensity of interhemispheric exchange among the models, these differences could not be adequately understood in terms of spatial distributions of tracer at the surface. Interhemispheric mixing has long been associated with north-south concentration gradients determined from observations, but the results suggested that the meridional gradient measured at the surface is a poor predictor of the true interhemispheric mixing time of a given model.

Both resolved transport and sub-grid scale "column physics" were important in determining the responses obtained by the models. Surprisingly, differences in the subgrid-scale parameterized transport appear to be at least as important in determining model performance as the differences between analyzed winds vs. calculated winds.

TransCom 3

The progress made in these first two phases of the TransCom project has been be directly applied to resolving some of the discrepancies in estimates of the global carbon budget. To this end, TransCom 3 involved a CO_2 inversion calculation intercomparison. Participating transport models were used to simulate the atmospheric response to an agreed-upon set of surface emission "basis functions" representing regional emissions and uptake of CO_2 due to various processes (industrial emissions, ecosystem metabolism, air-sea gas exchange, biomass burning, etc). The focus of this inversion intercomparison activity was to produce a formal estimate of the degree of uncertainty in such an inversion calculation that arises directly from the uncertainty in the model transport, the inversion methodology, and the observational data set used.

All levels of the TransCom 3 experiment have been completed: Level 1 annual mean inversion experiments; Level 2 seasonal cycle inversion experiments; and Level 3 interannual inversion inversion experiments. Results are still being generated and papers written that utilize the efforts made by all those that participated in the TransCom 3 experiment.

The results of TransCom 3, Level 1 annual mean inversion intercomprison have been published (Gurney et al., 2002), and data sensitivity analysis, model-to-model analysis, and other annual mean sensitivity work have been performed (Gurney et al., 2003; Law et al., 2003). The Level 2 cyclostationary control inversion intercomparison has been completed (Gurney et al., 2004; Gurney et al., 2005). The Level 3 interannual control inversion experiment has been completed (Baker et al., 2006) and other results are now being written.

This data set provides the results of the TransCom 3, Level 1 annual mean inversion experiments. The results from TransCom 3 Level 2 (seasonal) and Level 3 (interannual) inversion experiments will be archived by ORNL DAAC at a later date.

- **Methods and Materials:**

TransCom 3, Level 1 Models

Table 1. Atmospheric Tracer Transport Models Participating in TransCom 3, Level 1

Model	Modeler	Winds	H. Res.	# Levels	Advection	Subgrid	References
CSU[1]	Gurney & Denning	Online	72 lon. x 44 lat.	17 sigma	2nd order	Cum. mass flux (Arakawa & Schubert, 1974; Randall & Pan, 1993; Ding et al., 1998), var. prog. PBL (Suarez et al., 1983; Randall et al., 1992	Denning et al. (1996)
UCB[2]	Fung & John	1 h GISS GCMII'	72 lon. x 46 lat.	9 sigma	Slopes (Russell & Lerner, 1981)	Penetrative mass flux	Hansen et al. (1997)
UCI (s,b)[3]	Prather, Pak, Lee & Hannegan	GISS GCMII'	72 lon. x 46 lat.	9 sigma & 23 sigma	2nd order moments (Prather, 1986)	Penetrative mass flux w/updrafts, downdrafts and entrainment; diurnally varying PBL	Prather et al. (1987); Hansen et al. (1997); Koch & Rind (1998)
JMA	Maki	6 h JMA (1997)	144 lon. x 73 lat.	32 hybrid	Hor: semi-lag., Vert: box scheme	Vert diff. (Mellor-Yamada, Level 2.0), Cumulus (simple diff.) PBL (fixed layer)	Taguchi (1996)
MATCH: CCM3	Bruhwiler	NCAR CM3	128 lon. x 64 lat.	28 sigma	Spitfire	Corrective transport, subgrid diff., PBL w/stable mixing, cloud prediction	Rasch et al. (1997)
MATCH: NCEP	Chen	6 h NCEP (1990)	128 lon. x 64 lat.	28 sigma	Spitfire	Vert. diff. w/ diagnosed PBL; penetrative conv. + local conv. correction (Hack, 1994)	Rasch et al. (1997)

MATCH: MACCM2	Law	6 h MACCM2	64 lon. x 64 lat.	24 hybrid	Semi-lagrangian	Hack convection (Hack, 1994); vert. diff. w/ PBL (Holtslag & Boville, 1993)	Rasch et al. (1997); Law & Rayner (1999)
NIES	Maksyutov	12 h ECMWF (1997)	144 lon. x 72 lat.	15 sigma	Semi-lagrangian	Vert. diff. in troposphere (Hack, 1993); penetrative mass flux (Tiedke, 1989); vert. diff in PBL (Schubert at al., 1993)	Maksyutov & Inoue (2000)
NIRE CTM-96[4]	Taguchi	6 h ECMWF (1995)	144 lon. x 73 lat.	15 hybrid	Semi-lagrangian	Vert. diff in PBL, reduced diffusion at tropospause	Taguchi (1996)
RPN-SEF	Yuen & Higuchi	Online	128 lon. x 64 lat.	27 sigma	Semi-lag. (Richie & Beaudoin, 1994)	Vertical diffusion; PBL based on turbulent KE (Benoit et al., 1997)	D'Andrea et al. (1998)
SKYHI[2,5]	Fan	Online	100 lon. x 60 lat.	40 hybrid	2nd order	Dry/moist convective adjustment for T, q; non-local parameterization for vert. mixing in PBL	Mahlman et al. (1994); Strahan & Mahlman (1994)
TM2[6]	Bousquet & Peylin	12 h ECMWF (1990)	48 lon. x 24 lat.	9 sigma	Slopes (Russell & Lerner, 1981)	Mass flux (Tiedke, 1989); stability dependent vertical diffusion (Louis, 1979)	Heimann (1995); Bousquet et al. (1999)
TM3[2]	Heimann	6 h ECMWF (1990)	72 lon. x 45 lat.	19 hybrid	Slopes (Russell & Lerner, 1981)	Mass flux (Tiedke, 1989); stability dependent vertical diffusion (Louis, 1979, updated)	Heimann (1995)
GCTM[6]	Baker	6 h ZODIAC GCM	256 km2	11 sigma	2nd/4th order	Vert. diffusion, Ri number-based vert. mixing in lowest 3 layers to represent PBL	Mahlman & Moxim (1978); Levy et al. (1982)
CSIRO-CC[7]	Kowalczyk & McGregor	Online	208 km2	18 sigma	Hor: semi-alg (McGregor, 1996); Vert: total var diminishing	Stability dep. Vert diff. (Louis, 1979) + non-local scheme, mass flux conv. w/downdrafts	McGregor & Dix (2001)

Notes: [1]Participated in TransCom 1 and TransCom 2 but model differed.
[2]Participated in TransCom 2.
[3]UCI primary model uses 3-hourly GISS II' 9-layer GCM winds and is primarily tropospheric; UCIb is a boundary-layer variant with PBL height diagnosed from Ri number, super-resolved tracer gradients using second-order moments, and non-local closure on the subgrid (Hartke and Rind, 1997); UCIs uses 6-hourly GISS II' middle atmosphere GCM winds with a well resolved stratosphere (Koch and Rind, 1998).
[4]Earlier model version participated in TransCom 1, current model version in TransCom 2.
[5]A non-local parameterization for vertical mixing in the PBL was implemented after TransCom 2 and was used in TransCom 3.
[6]Participated in TransCom 1 and TransCom 2 with current model.
[7]Model output fields were interpolated from model's conformal-cubic grid to regular (2ßê latitude, longitude) grid before submission.

TransCom 3, Level 1 Basis Function Map

The investigators constructed a basis function map for the TransCom 3, Level 1 experiment that reflects both geographical and mechanistic elements. The terrestrial and oceanic portions of the world were each broken into 11 separate source/sink regions. The terrestrial boundaries were constructed following certain land use type classifications with some additional smoothing of the boundaries. Information about how the basis map was constructed, the basis function data file and a readme, the final smoothed basis map, and the GLOBALVIEW stations overlaid on the basis function map are provided in the compressed <**basis_function_map_all.zip**> file at the ORNL DAAC FTP area for TransCom3, Level 1. Uncompressed, the files are:

File name	Description
basis_map_construction.pdf	Explanation of the methodology used to construct the basis function map
smoothmap.fix.2.bin	Basis function data file
smoothmap.readme	Readme for basis function data file
make.map.new.f	A spatial smoother routine used to generate source/sink regions with smooth, continuous boundaries
newmap.adj.jpg	Original Unsmoothed Boundaries Map: Terrestrial regions, no smoothing applied
smoothmap2.final.2.jpg	Final Smoothed Basis Map: Terrestrial and oceanic regions with 2 smoothing passes
supp.figure.1.jpg	GLOBALVIEW CO_2 stations overlaid on the basis function map

The original unsmoothed boundaries and the final smoothed basis maps are shown below.

- **Original Unsmoothed Boundaries Map: Terrestrial Regions, No Smoothing Applied**

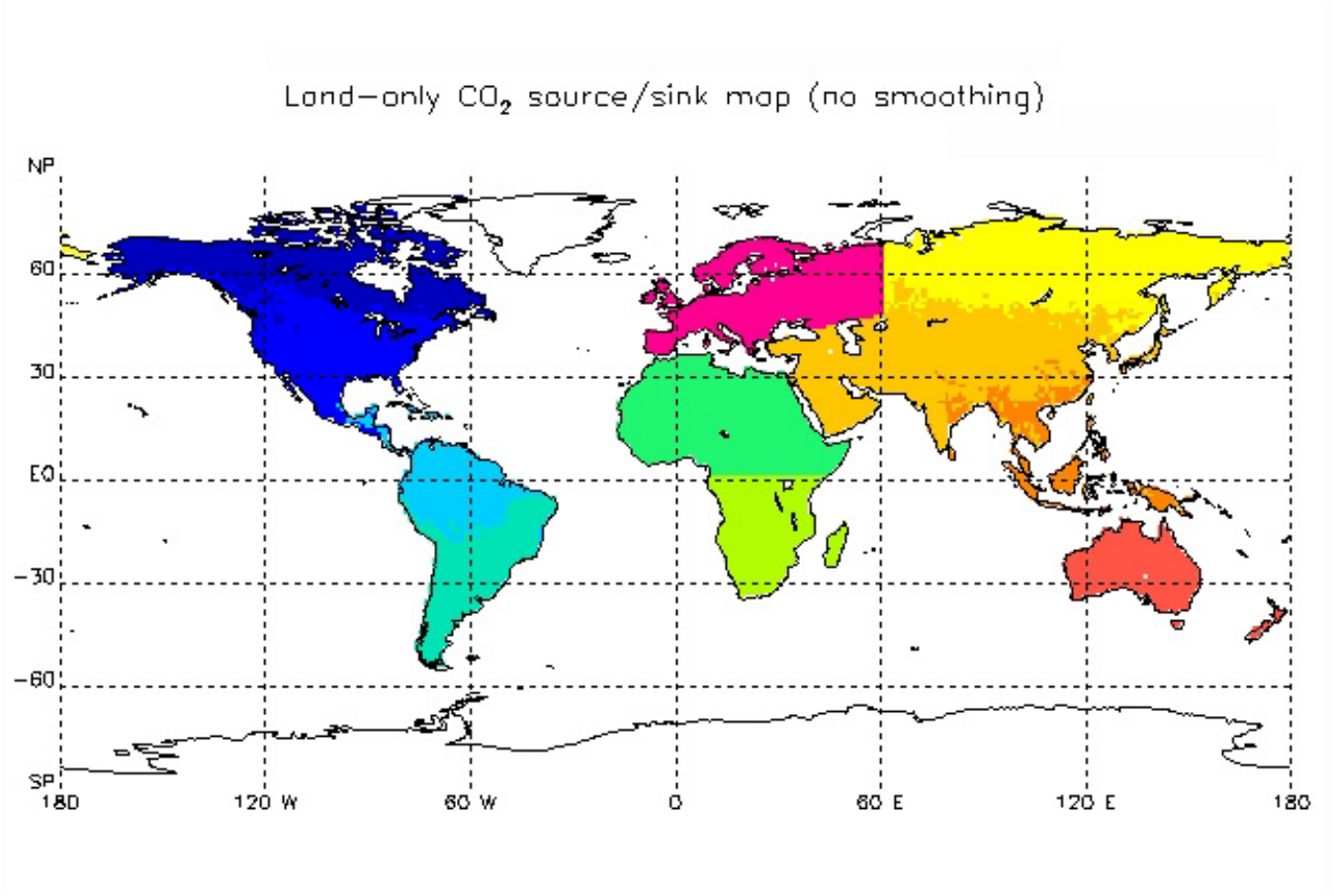

Final Smoothed Basis Map: Terrestrial and Oceanic Regions with 2 Smoothing Passes

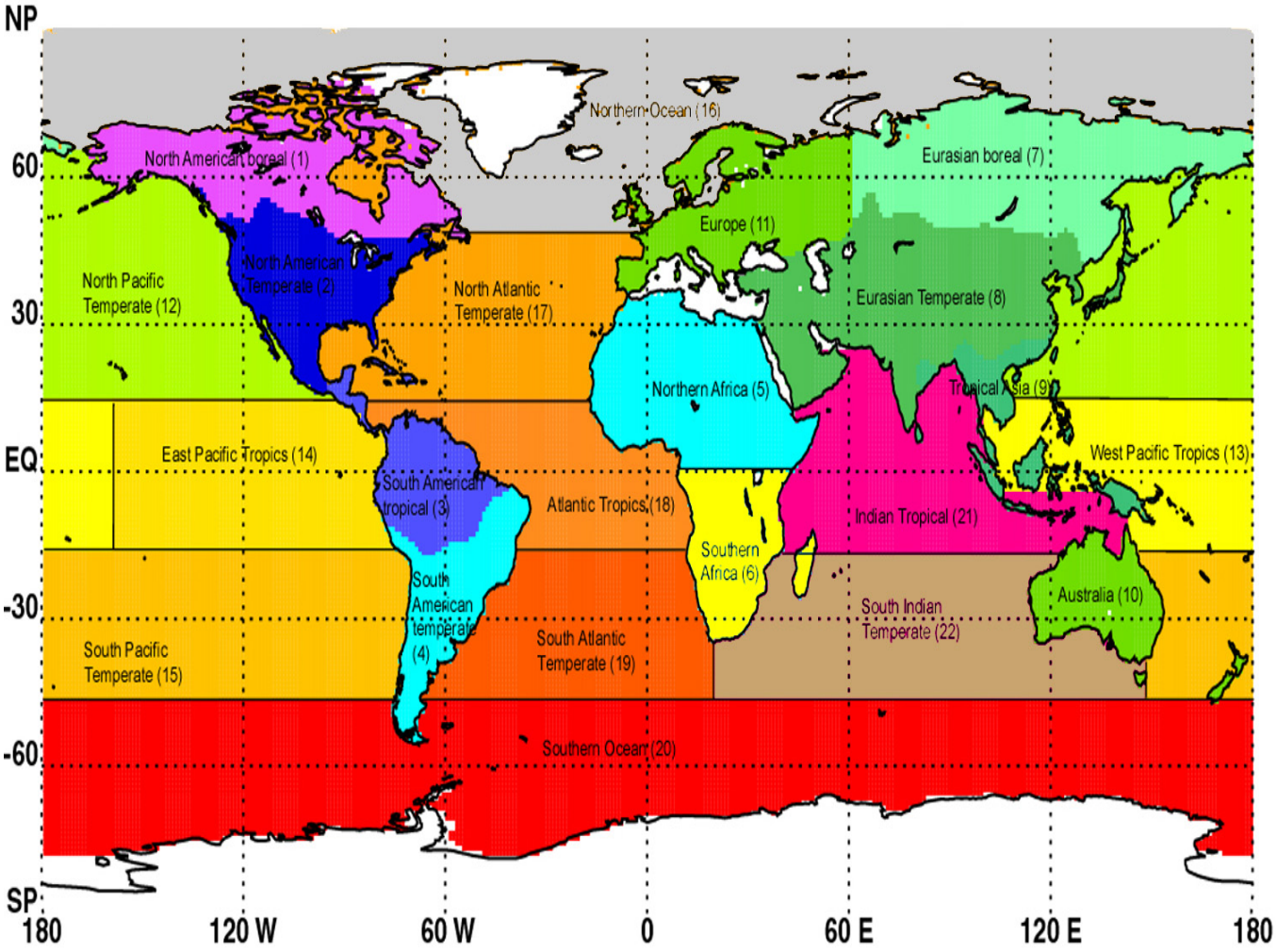

The investigators also provided a sea ice mask in the oceanic basis regions. Because of the substantial seasonality in sea ice extent, this imparted seasonal spatial structure to four of the oceanic basis regions. Follow this link to the sea ice mask discussion.

Data Collection:

TransCom 3, Level 1 Protocol

Contributors to TransCom 3, Level 1 followed a detailed experimental protocol (Gurney et al., 2000). The protocol file <**transcom3_level 1_experimental_protocol.pdf**> can be downloaded from the ORNL DAAC FTP / comp/ subdirectory for TransCom3, Level 1. The protocol is summarized below.

A. Forward Simulations: Level I Annual Mean Inversion (37 individual tracers)

The annual mean inversion consisted of a 4-year forward simulation (365 days per year) containing 4 pre-subtracted tracers, 11 sulfur hexafluoride (SF_6) tracers, and 22 CO_2 tracers (11 terrestrial, 11 oceanic).

1) Fossil-fuel carbon pre-subtraction

The supplied 1990 and 1995 fossil-fuel flux maps were run forward by each model for 4 years as two separate tracers. Since these maps represent the annual mean flux, no time interpolation was required - the flux values at each grid cell were simply repeated every timestep for 4 years.

2) Neutral biosphere carbon pre-subtraction

The supplied mid-month NEP flux maps were run forward by each model for 4 years. This required running the provided maps in repetition for each of the 4 simulated years. These mid-month values were interpolated to, at least, daily fluxes.

3) Oceanic carbon exchange pre-subtraction

The supplied mid-month net oceanic carbon exchange maps were run forward by each model for 4 years. This required running the provided maps in repetition for each of the 4 simulated years. These mid-month values were interpolated to, at least, daily fluxes.

4) Terrestrial carbon basis functions

The supplied terrestrial carbon basis function flux maps were run forward by each model for 4 years as 11 separate tracers. Since these maps contain no seasonality, no time interpolation was required - the flux values at each grid cell were simply repeated every timestep for 4 years.

5) Oceanic carbon basis functions

The supplied oceanic carbon basis function flux maps were run forward by each model for 4 years as 11 separate tracers. Unlike the terrestrial carbon basis function flux maps, the oceanic maps contain seasonality (due to changing ice cover in polar regions) and have been supplied as 12 monthly maps for each oceanic region.[1] The impact of ice cover is small and only impacts four of the oceanic regions, therefore no time interpolation was required - flux values at each grid cell were held at their month-specific value for each month period.

6) SF_6 basis functions

The supplied SF_6 basis function flux maps were run forward by each model for 4 years as 11 separate tracers. Since these maps represent the annual mean flux, no time interpolation was required - the flux values at each grid cell were simply repeated every timestep for 4 years.

---

[1] The ice cover map used in the construction of the oceanic carbon basis functions may not match the ice cover map implicit in offline model wind fields or used explicitly within online models. Correcting this would be extremely difficult, so it was left as part of the "model-to-model" difference.

B. Input Data Set Description:

The TransCom3 Level 1 input data set comprises all the data necessary to initiate the forward runs in the Level 1 experiment. This file contains seven records, each of which is a distinct tracer category. The file is a binary format and all variables are double precision (sample code with which to read the input data is supplied in the next section). Because investigators needed to ensure that all participants had precisely the same input fluxes, double precision was used for the input file so as to maintain precision in checking the global totals (see section E). The input data can be downloaded in compressed form as <**input_data_all.zip**> from the ORNL DAAC FTP /data/

subdirectory for TransCom 3, Level 1. This file contains:

File name	Description
input.new.le.dat.gz	The Level 1 input data set.
takahashi_data.pdf	Information about the net oceanic pre-subtraction carbon exchange maps (see #3 below).
statlocs.dat	CO2 monitoring station list (ascii file to facilitate insertion into model code). Includes 245 station locations.
read.statlocs.f	A short fortran program that reads the station location data.

All the input arrays represent 0.5 x 0.5 degree surface maps in which the first grid cell is centered at 89.75 S latitude, 179.75 W longitude, proceeding in the longitudinal direction. The grid arrangement is as follows:

i = 1 is centered at 179.75w, i increases eastward
j = 1 is centered at 89.75s, j increases northward

```
88.5s - | - - - | - - - | - - - | - -
        | (1,3) | (2,3) | (3,3) |

89s   - | - - - | - - - | - - - | - -
        | (1,2) | (2,2) | (3,2) |

89.5s - | - - - | - - - | - - - | - -
        | (1,1) | (2,1) | (3,1) |

90s -   | - - - | - - - | - - - |
    180w 179.5w 179w 178.5w
```

The data within the file <**input.new.le.dat.gz**> are described below.

1) 1990 and 1995 fossil-fuel pre-subtraction emission maps

The first two records are the fossil fuel pre-subtraction emission maps. They represent the annual mean emissions from fossil-fuel burning, hydraulic cement production, and gas flaring in 1990 and 1995, respectively. The emissions maps are shown here.

Description/Reference: The 1990 emissions map is derived from the data prepared by Andres et al. (1997) and can be found (with detailed supporting information) at the CDIAC website: http://cdiac.ornl.gov/epubs/ndp/ndp058/ndp058.html.

The 1995 emissions map is derived from the data prepared by Brenkert (1998) and can be found (with detailed supporting information) at the CDIAC website: http://cdiac.ornl.gov/ndps/ndp058a.html.

Specifications: The original 1 x 1 degree maps were subsampled to 0.5 x 0.5 degree maps in which the first grid cell is centered at 89.75 S latitude, 179.75 W longitude, proceeding in the longitudinal direction. These first two records each contain arrays of dimension: 720 x 360.

Units: kg C/m^2/second.

2) Neutral biosphere pre-subtraction maps

The next record contains the net ecosystem production (NEP) pre-subtraction carbon exchange flux maps, one for each month. Neutral biospheric CO_2 exchange maps for July and December are shown here.

Description/Reference: The NEP maps come from a steady-state CASA model run (Randerson et al., 1997).

Specifications: The original 1 x 1 degree maps were subsampled to 0.5 x 0.5 degree maps in which the first grid cell is centered at 89.75 S latitude, 179.75 W longitude, proceeding in the longitudinal direction. This record contains an array of dimension: 720 x 360 x 12.

Units: kg C/m^2/second.

3) Ocean exchange pre-subtraction maps

The next record contains the net ocean pre-subtraction carbon exchange flux maps, one for each month. July, December, and the annual mean ocean exchange maps are shown here.

Reference: The net oceanic pre-subtraction carbon exchange maps were produced by Taro Takahashi, updated from T97 (Takahashi et al., 1999). Detailed information about this data is found in the file <**takahashi_data.pdf**> which is included in the <**input_data_all.zip**> file.

Specifications: The original 4 x 5 degree maps were subsampled to 0.5 x 0.5 degree maps in which the first grid cell is centered at 89.75 S latitude, 179.75 W longitude, proceeding in the longitudinal direction. This record contains an array of dimension: 720 x 360 x 12.

Units: kg C/m^2/second.

4) Terrestrial carbon basis functions

The next record contains the terrestrial carbon basis function flux maps, one for each terrestrial region. The North American Temperate basis function and the NPP map are shown here.

Reference: The terrestrial carbon basis function flux maps represent the terrestrial portion of the normalized surface fluxes. These are the fluxes that are "adjusted" in the inverse portion of the TransCom 3 experiment in order to minimize the difference between the observed and simulated tracer concentrations. Each map represents a particular terrestrial region in which the annual summed flux over the region is equal to 1 Gt C/year. The flux from grid cells outside of a particular region is zero. The spatial distribution of the flux reflects annual mean NPP distribution as provided by a steady-state run of the model CASA (contact Jim Randerson for more information on the NPP map).

Specifications: The original NPP 1 x 1 degree maps were subsampled to 0.5 x 0.5 degree maps in order to create regional unit fluxes. The first grid cell is centered at 89.75 S latitude, 179.75 W longitude, proceeding in the longitudinal direction. This record contains an array of dimensions: 720 x 360 x 11. Note that the third dimension is the region index.

Units: kg C/m^2/second.

5) Ocean carbon basis functions

The next record contains the ocean basis function flux maps, one for each ocean region and month. The January North Pacific Temperate basis function and the global July and January sea ice maps are shown here.

Reference: The monthly ocean basis function flux maps represent the oceanic portion of the normalized surface fluxes. These are the fluxes that are "adjusted" in the inverse portion of the TransCom 3 experiment in order to minimize the difference between the observed and simulated tracer concentrations. Each map represents a particular ocean region and particular month combination in which the annual summed flux over a region is equal to 1 Gt C/year.

There is no spatial distribution to the flux with the exception of seasonal ice cover in those areas for which ice cover occurs (changing ice cover is the motivation for monthly maps). The sea ice cover data comes from the boundary conditions used by World Climate Research Programme, Working Group on Numerical Experimentation, Atmospheric Model Intercomparison Project (AMIP) (Taylor et al., 2001).

Specifications: The original ice cover 1 x 1 degree maps were subsampled to 0.5 x 0.5 degree maps in order to create regional/monthly unit fluxes. The first grid cell is centered at 89.75 S latitude, 179.75 W longitude, proceeding in the longitudinal direction. This record contains an array of dimensions: 720 x 360 x 11 x 12. Note that the third dimension is the region index, the fourth dimension is the month index.

Units: kg C/m^2/second.

6) SF_6 basis functions

The next record contains the SF_6 basis function flux maps, one for each land region. The SF_6 flux from the Europe basis function is shown here.

Reference: The SF_6 basis function flux maps were used to invert for a flux whose global distribution is relatively well-known. The same 11 land basis function regions used for the unit carbon fluxes are utilized in the SF_6 flux maps. Each map represents a particular land region in which the annual summed flux over the region is equal to 1 Gg SF_6/year.

Specifications: The spatial distribution of the SF_6 flux is similar to that used in TransCom 2. In the present experiment, the spatial distribution has been scaled such that the flux in each basis function region sums to 1 Gg SF_6/year.

The spatial distribution of the SF_6 flux was constructed as described in Denning et al., 1999. The first grid cell is centered at 89.75 S latitude, 179.75 W longitude, proceeding in the longitudinal direction. This record contains an array of dimensions: 720 x 360 x 11. Note that the third dimension is the region index.

Units: kg SF_6/m^2/second.

D. Reading the input data set and regridding:

Sample code[2]

****

This program reads the TransCom 3 input variables out of the binary input data file (input.new.le.dat.gz).

```
**********************************************************************

      Real*8, Dimension(720,360)          :: ff90,ff95
      Real*8, Dimension(720,360,11)       :: sf6,landunit
      Real*8, Dimension(720,360,12)       :: nep,ocean
      Real*8, Dimension(720,360,11,12)    :: oceanunit

      Open(unit=10,file='input.new.le.dat',form='unformatted')

      Read(10) ff90
      Read(10) ff95
      Read(10) nep
      Read(10) ocean
      Read(10) landunit
      Read(10) oceanunit
      Read(10) sf6

      Close(10)
```

Participants spatially aggregated to their model grid for forward runs at this point

```
     Stop
     End

**********************************************************************
```

•

---

[2] The input data are read and carried as double precision in order to match the global sums specified in Section E below. The precision with which each model carries out the forward integrations is an individual decision. However, output reporting is required in single precision.

Spatial aggregation

1) Land/sea boundary

Spatial aggregation of the input fields onto model grids raises some particularly difficult problems at the land/sea boundary. Given a terrestrial input carbon flux field, such as fossil fuel emissions, some of the smaller 0.5 x 0.5 degree gridcells may lie in what a particular model land/sea mask may designate as an ocean gridcell. The approach investigators took in TransCom2 to deal with this was to simply take the amount of emissions found outside of the designated land area, and allocate it evenly across the entire land area such that the global totals matched those computed with the 0.5 x 0.5 degree map. However, this can cause unfortunate spatial redistribution of input fluxes that have maxima near coastlines where large vertical transport gradients occur. Investigators decided upon a method to solve this problem that is easy and best maintains the spatial pattern of the input fluxes (thanks to helpful input from Roger D., Rachel M., and Peter R.).

There are two steps to the procedure that was performed for each input field reaggregation:

a) All of the 0.5 x 0.5 degree cells from each input field were placed within the confines of (larger) model

gridcells. For most modelers, the 0.5 x 0.5 degree size fit evenly within the model gridcell (that is, most grids lie on whole or half degree lines). For those grids for which this is not the case, the 0.5x0.5 degree gridcells were apportioned by area to the model gridcells that they straddle.

This allocation of the 0.5 x 0.5 degree gridcells to the model grid was done while applying the land/sea mask that is routinely used with the model grid. So, all the gridcells that are considered "land" (in the case of the terrestrial pre-subtracted fields, for example) by the land/sea mask were filled by the 0.5 x 0.5 degree gridcells supplied in the input data. Refer to Figure 1 for a schematic of a coastline example.

Figure 1

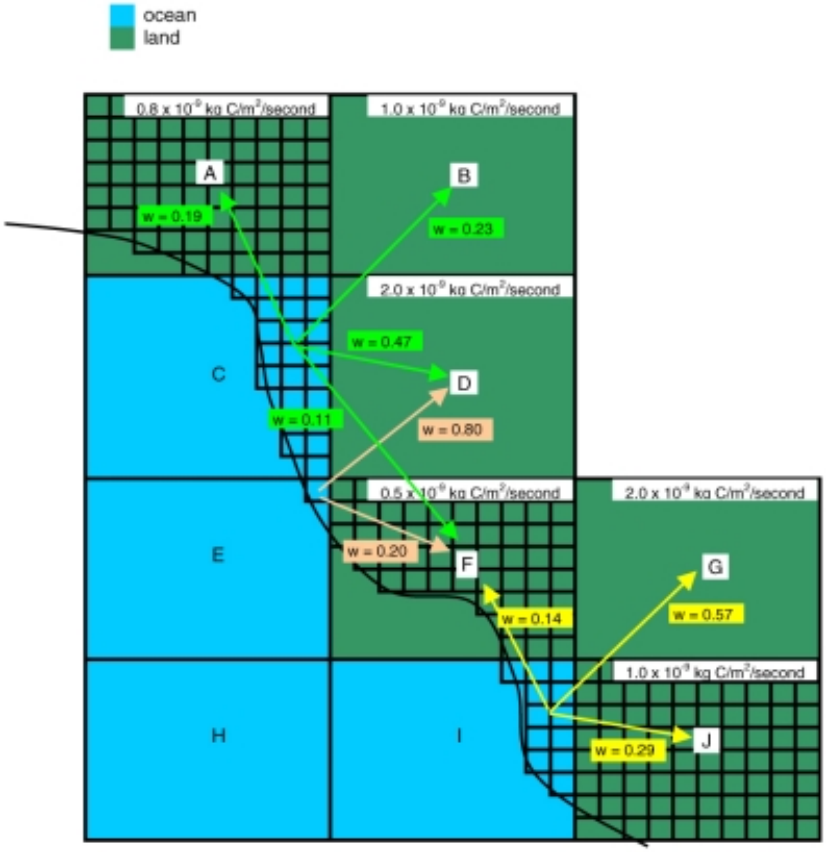

b) The next step was to go back over the two grids (the model grid and the 0.5 x 0.5 degree grid) and locate those model gridcells which contain emitting 0.5 x 0.5 degree gridcells but were allocated to ocean (while allocating a terrestrial pre-subtraction field, for example) or land (while allocating the ocean pre-subtraction field, for example). In these cases, the 0.5 x 0.5 degree gridcells in question had their integrated flux added to the neighboring model gridcells *a la* weights which reflected the relative flux from those neighbors. In Figure 1, 0.5 x 0.5 degree gridcells in model gridcell "C" are area integrated and added to the flux in the neighboring land model gridcells with the weights denoted by "w".[3]

The effect of this procedure was to keep the reallocation of emissions *local*. This is most obvious for the case of fossil-fuel emissions which have strong maxima near the coastlines - instead of potentially removing this maxima and redistributing it across the entire globe or region, the maxima is shifted inland slightly. It is an imperfect solution in the sense that flux minima located on a coastline are essentially lost with the reshuffling procedure. However, for the purposes here, the loss of a small local flux is of comparitively little consequence.

This procedure was performed for all of the input files except the ocean carbon basis functions. The ocean carbon basis function fields have essentially no spatial distribution (four of the basis functions have a bit of spatial structure due to seasonal sea ice cover) and therefore are best handled with the traditional approach. This was accomplished by eliminating those model gridcells that contain oceanic flux but which are considered land gridcells according to the land/sea mask. The region total is then scaled-up to match the annual, regional sum of 1 Gt C/year (see Section E).[4]

1) Region/region boundary

Another question concerning the spatial aggregation arises at boundaries between basis function regions. Unlike the land/ocean problem discussed above, there is no strict spatial mask to worry about (i.e., the land/sea mask of each model) and there are no obvious atmospheric transport gradients coinciding with any of the region/region boundaries. However, problems can arise since there is some significant spatial structure to the fluxes in the various regions (mainly the terrestrial basis functions and SF_6 basis functions).

The "soft" boundary approach was recommended for this experiment. This would result in region/region boundaries overlapping by, on average, half of a model gridcell. The integrated flux in each region, however, would be maintained. Since the basis function arrays have been constructed such that each array contains values only in each region and the remainder of the array contains zeros, this made the process very simple.

For each region (which are separate arrays in the input data file), modelers placed all of the 0.5 x 0.5 degree cells within the confines on their model gridcells. Model gridcells that contain even one 0.5 x 0.5 degree emitting gridcell were considered part of the new regridded region defined by the model grid. This maintained the total regional flux but spread the flux in the edge cells, on average, outward from the region by half of a model gridcell. Adjacent regions, overlapped in space slightly.

The other alternative might be referred to as a "hard" boundary in which there is no gridcell overlap: a model gridcell is in one region or another, not both. This moves the flux as with the "soft" approach but requires regional scaling and could cause significant alteration of the spatial structure of the flux were a region edge to contain high levels of flux.

These two approaches are shown below:

Figure 2

Imagine this as the nep flux in the vicinity of a regional boundary

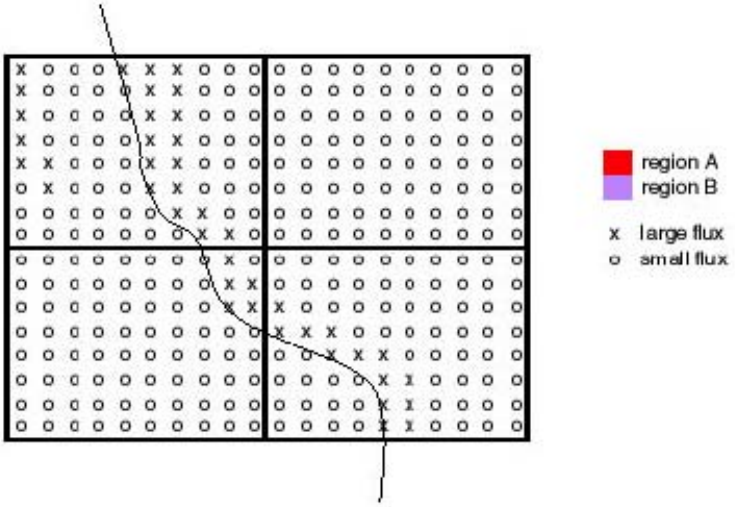

The arrays in input.dat only define fluxes within a given region

This flux that is not captured would be spread across region B according to the spatial distribution of the flux in the region.

HARD BOUNDARY

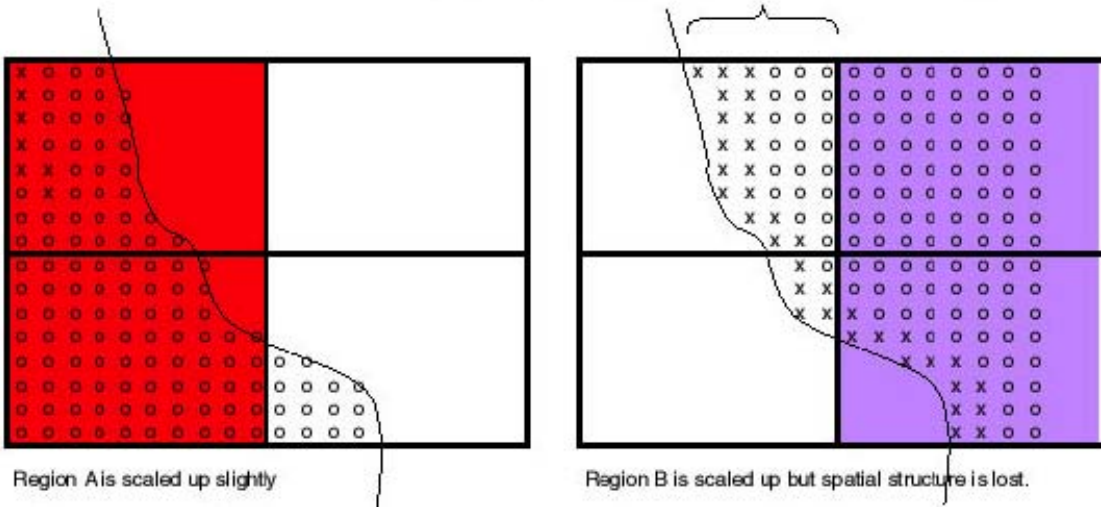

Region A is scaled up slightly

Region B is scaled up but spatial structure is lost.

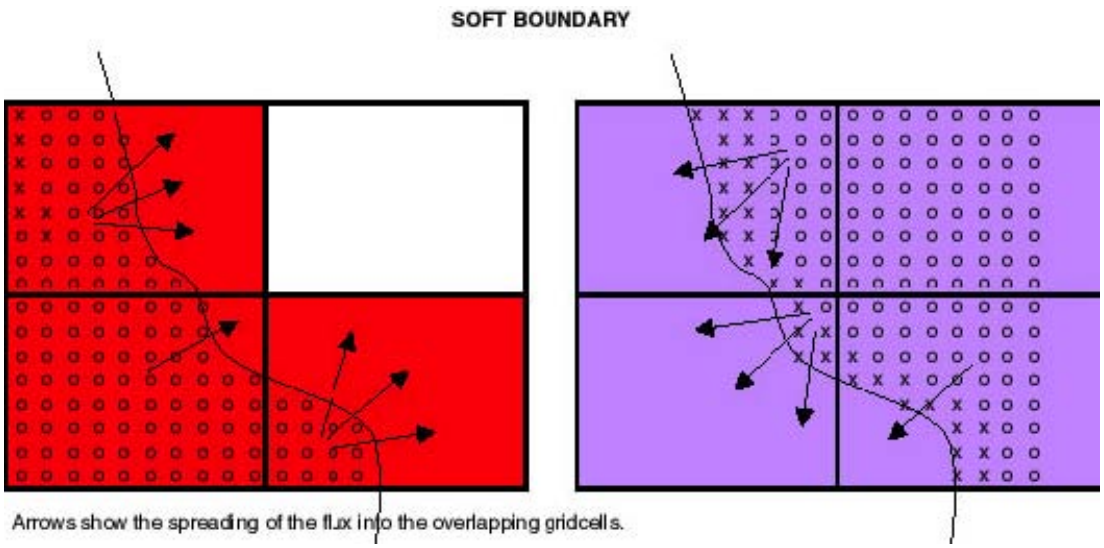

---

[3] Because many coastlines run roughly north-south, the order with which this shuffling scheme is performed does change the shuffling weights. For example, going from the South Pole and working northward will have a slightly different shuffling effect than going from the North Pole and working southward. Though, the effect is small, the investigators recommended that modelers determine the weights prior to reallocation - this eliminates the directional bias.

[4] Aside from the spatial flux pattern caused by sea ice cover (four regions only), further spatial patterning occurs due to the fact that some edge model gidcells are not be fully populated by 0.5 x 0.5 degree gridcells and, hence, have less flux than interior gridcells.

E. Maintaining global totals:

All of the input data was generated at 0.5 x 0.5 degree to facilitate interpolation to the various model grids involved in TransCom 3. It was important that whatever spatial aggregation was performed did not alter the global sums provided below. After the input data was spatially aggregated to each model grid, modelers made sure that their global totals matched those below through regional/global scaling adjustments. The global/regional sums are as follows[5]:

1) Fossil-fuel pre-subtraction maps

The total 1990 emissions are 5.811611 Gt
The total 1995 emissions are 6.172869 Gt

2) Neutral biosphere pre-subtraction maps

The following are Global Mid-month NEP Flux Values (in kg C/second). After spatial aggregation to model grids, modelers checked to ensure that their globally integrated mid-month fluxes matched the following:[6]

Month	Global Mid-month NEP Flux Values (kg C/second)

1	242859.5
2	314486.3
3	211004.9
4	251455.6
5	-148549.7
6	-607653.2
7	-755280.0
8	-384896.5
9	180157.9
10	261082.3
11	233356.8
12	201913.8

These mid-month fluxes were interpolated to, at least, daily fluxes using standard month lengths (31, 28, 31 days, etc.). After interpolation, the Globally Summed Monthly NEP Flux Totals (in Gt/month) matched the following:

Month	Global Monthly NEP Flux Value (Gt/month)
1	0.6644884
2	0.7098920
3	0.6139190
4	0.5037655
5	-0.4368679
6	-1.4607660
7	-1.8092093
8	-0.9421531
9	0.3264070
10	0.6634400
11	0.6024190
12	0.5654337

The Global Annual NEP Flux is: 7.6815368E-4 Gt/year

---

[5] The global sums represent: (flux value*m^2/gridcell*seconds/year{or month}) summed over all grid cells.

[6] Assuming the fluxes represent mid-month values when initially derived as monthly means will lead to a different time integral. For the purposes of TransCom, however, the important requirements were that (1) everybody used the same daily flux and (2) the global annual flux in the mid-month daily interpolated version was

not drastically different from the original monthly mean version. These were satisfied by adhering to the procedure and global totals listed.

3) Ocean exchange pre-subtraction maps

The following are Global Mid-month Oceanic Exchange Values (in kg C/second). After spatial aggregation to model grids, modelers checked to ensure that their globally integrated mid-month fluxes matched the following (see footnote 4):

Month	Global Mid-month Oceanic Exchange Values (kg C/ second)
1	-78500.75
2	-71361.29
3	-75480.51
4	-76880.54
5	-77084.09
6	-69717.96
7	-47504.78
8	-46194.30
9	-53969.30
10	-71638.83
11	-79507.18
12	-86656.08

These mid-month fluxes were interpolated to, at least, daily fluxes using standard month lengths (31, 28, 31 days, etc.). After interpolation, the Globally Summed Monthly Oceanic Exchange Totals (in Gt/month) matched the following:

Month	Global Monthly Oceanic Exchange Values (Gt/month)
1	-0.2101370
2	-0.1758068
3	-0.2013174
4	-0.1989271
5	-0.2037262
6	-0.1753489
7	-0.1338484
8	-0.1269569
9	-0.1435823
10	-0.1890994
11	-0.2061724

12	-0.2269120

The Global Annual Ocean Flux is: -2.191835 Gt/year

4) Terrestrial carbon basis functions

The Global Total Flux for each region is 1.0 Gt/year

5) Oceanic carbon basis functions

The Global Total Flux for each region is 1.0 Gt/year

6) SF_6 basis functions

The Global Total Flux for each region is 1.0 Gg/year

Product Description and Data File Information:

TransCom 3, Level 1 Results

The results of the TransCom 3, Level 1 experiments are grouped into two broad categories:

- Forward simulation fields and response functions ("model output")
- Estimated fluxes ("inversion results")

A. Level 1 Model Output

1) **Selected CO_2 Fields from All of the Submitted Models**

These image files can be downloaded in compressed form as <**model_results_co2_fields_all.zip**> from the ORNL DAAC FTP area for TransCom 3, Level 1. Uncompressed, the files provide three different types of model output:

- Annual Mean Surface Concentration (.jpg maps)

Description	Model Set 1 File Names	Model Set 2 File Names
1990 fossil fuel	L1.ff90_s.annmn.1.jpg	L1.ff90_s.annmn.2.jpg
Neutral biosphere	L1.bios_s.annmn.1.jpg	L1.bios_s.annmn.2.jpg
Ocean exchange	L1.ocean_s.annmn.1.jpg	L1.ocean_s.annmn.2.jpg
Land BF 2	L1.landBF2_s.annmn.1.jpg	L1.landBF2_s.annmn.2.jpg

Ocean BF 5	L1.oceanBF5_s.annmn.1.jpg	L1.oceanBF5_s.annmn.2.jpg
Predicted surface concentration	L1.pred_s.annmn.1.jpg	L1.pred_s.annmn.2.jpg

Note: In the file name, ...1.jpg refers to Model Set 1 results and ... 2.jpg refers to Model Set 2 results. Model Set 1: CSU, UCB, UCI, UCIb, UCIs, JMA, MATCH:CCM3, MATCH:NCEP. Model Set 2: MATCH:MACCM2, NIES, NIRE, RPN, SKYHI, TM2, TM3, GCTM. Each field uses a single scale unless noted otherwise.

- Annual Mean Cross-sections (.jpg plots)

Description	Model Set 1 File Names	Model Set 2 File Names
1990 fossil fuel	L1.ff90.annmn.xsect.1.jpg	L1.ff90.annmn.xsect.2.jpg
Neutral biosphere	L1.bios.annmn.xsect.1.jpg	L1.bios.annmn.xsect.2.jpg
Ocean exchange	L1.ocean.annmn.xsect.1.jpg	L1.ocean.annmn.xsect.2.jpg
Land BF 9	L1.landBF9.annmn.xsect.1.jpg	L1.landBF9.annmn.xsect.2.jpg
Ocean BF 9	L1.oceanBF9.annmn.xsect.1.jpg	L1.oceanBF9.annmn.xsect.2.jpg

Note: In the file name, ...1.jpg refers to Model Set 1 results and ... 2.jpg refers to Model Set 2 results. Model Set 1: CSU, UCB, UCI, UCIb, UCIs, JMA, MATCH:CCM3, MATCH:NCEP. Model Set 2: MATCH:MACCM2, NIES, NIRE, RPN, SKYHI, TM2, TM3, GCTM. Each field uses a single scale unless noted otherwise.

- Annual Mean Surface Zonal Means (.pdf charts)

Description	File Name
1990/1995 fossil fuel	L1.ff_s.zonalmean.annmn.pdf
Neutral biosphere	L1.bios_s.zonalmean.annmn.pdf
Ocean exchange	L1.ocean_s.zonalmean.annmn.pdf
Land BF 9	L1.landBF9_s.zonalmean.annmn.pdf
Ocean BF 9	L1.oceanBF9_s.zonalmean.annmn.pdf

2) **High-frequency Station CO_2 Concentration Output**

These files contain the first 228 station locations in the <**statlocs.dat**> file. The remaining 17 stations (Pacific Ocean stations) did not require high frequency reporting. Each data file includes an explanatory readme file. Each data file is tarred and compressed. They are approximately 40 MB each. All of the data files have been compressed into one zip file which can be downloaded as <**model_results_statco_all.zip**> from the ORNL DAAC FTP area for TransCom 3, Level 1. The data files are:

CSIRO.cc.L1.statco2.le.tar.gz	CSU.gurney.L1.statco2.le.tar.gz
GCTM.baker.L1.statco2.le.tar.gz	GISS.fung.L1.statco2.le.tar.gz
GISS.prather.L1.statco2.le.tar.gz	GISS.prather2.L1.statco2.le.tar.gz
GISS.prather3.L1.statco2.le.tar.gz	JMA-CDTM.maki.L1.statco2.le.tar.gz
MATCH.bruhwiler.L1.statco2.le.tar.gz	MATCH.chen.L1.statco2.le.tar.gz
MATCH.law.L1.statco2.le.tar.gz	NIES.maksyutov.L1.statco2.le.tar.gz
NIRE.taguchi.L1.statco2.le.tar.gz	RPN.yuen.L1.statco2.le.tar.gz
SKYHI.fan.L1.statco2.le.tar.gz[7]	TM2.lsce.L1.statco2.le.tar.gz
TM3.heimann.L1.statco2.le.tar.gz	

[7] No high-frequency data was submitted - this data set has been created using the monthly mean data in those grid cells occupied by the T3 stations.

3) **Annual Mean Response for All Stations and Tracers**

These ASCII (.dat) data files provide response functions for 245 stations and 26 tracers. The first two lines contain explanatory information, the following 246 contain the response functions at each station/tracer, the last line contains an additional line for closing the atmospheric carbon budget. The data files can be downloaded in compressed form as <**model_results_gmatrices_all.zip**> from the ORNL DAAC FTP area for TransCom 3, Level 1. The data files are:

CSU.gurney.Gmat.dat	GCTM.baker.Gmat.dat
GISS.fung.Gmat.dat	GISS.prather.Gmat.dat
GISS.prather2.Gmat.dat	GISS.prather3.Gmat.dat
JMA-CDTM.maki.Gmat.dat	MATCH.bruhwiler.Gmat.dat
MATCH.chen.Gmat.dat	MATCH.law.Gmat.dat
NIES.maksyutov.Gmat.dat	NIRE.taguchi.Gmat.dat
RPN.yuen.Gmat.dat	SKYHI.fan.Gmat.dat[8]

TM2.lsce.Gmat.dat	TM3.heimann.Gmat.dat

[8] No high-frequency data was submitted - this data set has been created using the monthly mean data in those gridcells occupied by the T3 stations.

4) **Grid Information Files**

These are self-explanatory ASCII (.info) files. The files can be downloaded in compressed form as <**model_results_surfdat_all.zip**> from the ORNL DAAC FTP area for TransCom 3, Level 1. The data files are:

CSU.gurney.grid.info	GCTM.baker.grid.info
GISS.fung.grid.info	GISS.prather.grid.info
GISS.prather2.grid.info	GISS.prather3.grid.info
JMA-CDTM.maki.grid.info	MATCH.bruhwiler.grid.info
MATCH.chen.grid.info	MATCH.law.grid.info
NIES.maksyutov.grid.info	NIRE.taguchi.grid.info
RPN.yuen.grid.info	SKYHI.fan.grid.info
TM2.lsce.grid.info	TM3.heimann.grid.info

5) **SF_6 Surface Concentrations**

These are binary (.dat) files containing an array dimensioned as lon x lat x land BF (11) x month (12). For the lon and lat dimensions, check the grid information files above. The files can be downloaded in compressed form as <**model_results_sf6_all.zip**> from the ORNL DAAC FTP area for TransCom 3, Level 1. The data files are:

CSIRO.cc.L1.sf6.le.dat.gz	CSU.gurney.L1.sf6.le.dat.gz
GCTM.baker.L1.sf6.le.dat.gz	GISS.fung.L1.sf6.le.dat.gz
GISS.prather.L1.sf6.le.dat.gz	GISS.prather2.L1.sf6.le.dat.gz
GISS.prather3.L1.sf6.le.dat.gz	JMA-CDTM.maki.L1.sf6.le.dat.gz
MATCH.bruhwiler.L1.sf6.le.dat.gz	MATCH.chen.L1.sf6.le.dat.gz
MATCH.law.L1.sf6.le.dat.gz	NIES.maksyutov.L1.sf6.le.dat.gz
NIRE.taguchi.L1.sf6.le.dat.gz	RPN.yuen.L1.sf6.le.dat.gz
SKYHI.fan.L1.sf6.le.dat.gz	TM2.lsce.L1.sf6.le.dat.gz
TM3.heimann.L1.sf6.le.dat.gz	

6) **3D Monthly Mean Concentrations**

These are binary files containing an array dimensioned as: lon x lat x pressure level (9) x month (12) x BF (26). For the lon and lat dimensions, check the grid information files above. The "26" is the total number of tracers (4 background + 22 basis functions). Each data file is compressed. All of the data files have been compressed into one zip file which can be downloaded as <**model_results_mmean_3D_all.zip**> from the ORNL DAAC FTP area for TransCom 3, Level 1. The data files are:

CSIRO.cc.L1.mmean.le.3D.gz	CSU.gurney.L1.mmean.le.3D.gz
GCTM.baker.L1.mmean.le.3D.gz	GISS.fung.L1.mmean.le.3D.gz
GISS.prather.L1.mmean.le.3D.gz	GISS.prather2.L1.mmean.le.3D.gz
GISS.prather3.L1.mmean.le.3D.gz	JMA-CDTM.maki.L1.mmean.le.3D.gz
MATCH.bruhwiler.L1.mmean.le.3D.gz	MATCH.chen.L1.mmean.le.3D.gz
MATCH.law.L1.mmean.le.3D.gz	NIES.maksyutov.L1.mmean.le.3D.gz
NIRE.taguchi.L1.mmean.le.3D.gz	RPN.yuen.L1.mmean.le.3D.gz
SKYHI.fan.L1.mmean.le.3D.gz	TM2.lsce.L1.mmean.le.3D.gz
TM3.heimann.L1.mmean.le.3D.gz	

7) **2D Monthly Mean Concentrations**

These are binary files containing an array dimensioned as: lon x lat x month (12) x BF (26) x index. For the lon and lat dimensions, check the grid information files above. The "26" is the total number of tracers (4 background + 22 basis functions). The index number refers to either the surface ("1") or the layer above the surface ("2"). Each data file is compressed. All of the data files have been compressed into one zip file which can be downloaded as <**model_results_mmean_2D_all.zip**> from the ORNL DAAC FTP area for TransCom 3, Level 1. The data files are:

CSIRO.cc.L1.mmean.le.2D.gz	CSU.gurney.L1.mmean.le.2D.gz
GCTM.baker.L1.mmean.le.2D.gz	GISS.fung.L1.mmean.le.2D.gz
GISS.prather.L1.mmean.le.2D.gz	GISS.prather2.L1.mmean.le.2D.gz
GISS.prather3.L1.mmean.le.2D.gz	JMA-CDTM.maki.L1.mmean.le.2D.gz
MATCH.bruhwiler.L1.mmean.le.2D.gz	MATCH.chen.L1.mmean.le.2D.gz
MATCH.law.L1.mmean.le.2D.gz	NIES.maksyutov.L1.mmean.le.2D.gz
NIRE.taguchi.L1.mmean.le.2D.gz	RPN.yuen.L1.mmean.le.2D.gz
SKYHI.fan.L1.mmean.le.2D.gz	TM2.lsce.L1.mmean.le.2D.gz
TM3.heimann.L1.mmean.le.2D.gz	

B. Level 1 Inversion Results:

A “control” or “base” case inversion was performed with the Level I model output submissions. The investigators employed a Bayesian synthesis inversion formalism, specifying prior estimates of both the fluxes and their

uncertainty, and optimizing with respect to atmospheric observations which are also uncertain.

1) **Output Files**

All the ingredients and the basic inversion output, including basic output files generated by the IDL inverse code, have been compressed into one zip file which can be downloaded as <**inversion_results_invout_all.zip**> from the ORNL DAAC FTP area for TransCom 3, Level 1. The data files are:

File Name	Description
inversion.tar.Z	Inversion output files
outsum.allpre.dat	Model mean posterior fluxes for all 22 basis function regions and regional groupings. Also contains "within" and "between" uncertainties. All presubtraction fields are included.
outmod.allpre.dat	Individual model posterior fluxes and uncertainties.
outgrp.allpre.dat	Individual model results for the regional groupings.

2) **Basic Elements for the Inversion**

a) Data

The inversion is forced with 1992-1996 mean CO_2 concentration data calculated from GLOBALVIEW-CO_2 (2000). This data set encompasses 141 data records from 18 measuring programs including both flask and continuous measurements. Not all sites were operational during the full time period of interest but GLOBALVIEW uses a data interpolation/extrapolation scheme to fill data gaps and provide complete data records at all available observing sites. Since the CO_2 records contain both a trend and a seasonal cycle, the investigators choose here to use this interpolated data in calculating the 1992-1996 mean so that these values are not biased by missing portions of the data record. However the investigators rejected any site where the interpolated data was greater than 30% of the total data. Using this criterion, 76 sites were used in the inversion.

The data uncertainty needs to encompass a number of factors including measurement precision, network intercalibration, and the ability of the model to represent the observation and interannual variability. The investigators found that the inversion is sensitive to the choice of data uncertainty used. While the choice made here for the control inversion is not intended to be optimal, it is designed to incorporate a range of factors that impact the inversion through the data uncertainty specification. Previous inversions have used either constant uncertainties at all sites (with values ranging from 0.3-0.85 ppmv) or uncertainties which scale according to the variability at a site. Here we base the uncertainties on the residual standard deviation (rsd) given in GLOBALVIEW. This is a measure of the variability of individual flask samples around the smooth fitted curve from which the pseudo-weekly GLOBALVIEW data are generated. The rsd values are consequently higher for sites that are close to local, heterogeneous sources where data sets tend to be noisier. This, then, provides a measure of the uncertainty in modeling a particular location since we expect the modeling to be less reliable when close to sources.

The rsd values are modified in a number of ways to create the data uncertainties used here. The investigators describe the process and its justification as a series of steps that were applied to each site.

1. The GLOBALVIEW annual rsd values are averaged over 1992-1996.

2. When the inversion is performed, a data mismatch is generated for each site. The methodology assumes that these mismatches, normalized by the initial data uncertainty for that site, will be normally distributed with mean 0 and standard deviation of 1. Initial tests produced standard deviations that were too small, indicating data uncertainties that were too large. The investigators consequently reduced the rsd values by dividing by the square root of 5 multiplied by the proportion of "real" data contributed to the 1992-1996 mean. This effectively gives extra weight to those sites with more complete data records.

3. This also gives a number of sites with data uncertainties less than 0.3 ppmv. This is unrealistic, both due to intercalibration issues between measuring programs and modeling constraints associated with approximating site locations with grid box average concentrations. The investigators, therefore, set all data uncertainties to a minimum of 0.3 ppmv.

4. Finally, the observational network is spatially heteorogeneous. In the control case the investigators present here, there are some locations with multiple data records and large parts of the globe with no measurements. The investigators make some account for this heteorogeneity by giving less weight (i.e., larger data uncertainty) to data records that are co-located or close to each other, and do this by multiplying the data uncertainty for each site by the square root of the number of data records which are located within 4º latitude and longitude and 1000 m altitude of each other.

The data file used to force the inversion (**datafile.dat**) is included in the <**inversion_code_all.zip> file** (see below). The CO2 station list (**statlocs.dat**) is included in the <**input_data_all.zip**> file and a picture of the stations overlaid on the basis function map (**supp.figure.1.jpg**) in included in the <**basis_function_map_all.zip**> file. All of these files can be downloaded at the ORNL DAAC FTP area for TransCom3, Level 1.

b) Prior Fluxes and Uncertainties:

The prior flux estimates for the terrestrial basis functions represent an average of recent inventory studies.

Table 2. Prior Flux Estimates by Region

Region	Prior Flux (Gt C/year)
North American Boreal	0.0
North American Temperate	-0.2
Tropical America	0.55
South American Temperate	0.0
Northern Africa	0.15
Southern Africa	0.15
Boreal Asia	-0.4

Temperate Asia	0.3
Tropical Asia	0.8
Australia	0.0
Europe	-0.1

The prior flux uncertainties for the terrestrial basis function regions were equivalent to the growing season net flux (GSNF, defined as the sum of carbon uptake for all months in which this was a positive number) as provided by the CASA model of net ecosystem production.

Oceanic prior fluxes are set at zero for each oceanic region. Ocean source uncertainties are based on density of pCO2 measurements and the area of each region.

The prior flux file is included in the compressed file <**inversion_code_all.zip**> (see below).

c) Inversion Code:

The inversion code and related files can be downloaded as <**inversion_code_all.zip**> at the ORNL DAAC FTP area for TransCom3, Level 1. The files are described below:

File Name	Description
transcom.pro	The inversion code used for the Level I inversion.
control.dat	The control file required by the inversion code.
datafile.dat	The data file used to force the inversion.
prior.flux.dat	The prior flux file.

The inversion code used for the Level I inversion was developed by Peter Rayner with further work by Rachel Law and Kevin Gurney. It is written in IDL. In addition to the observational data and the prior flux/uncertainties, this code requires the control file which contains paths to the model response functions (see model output section), direction on which pre-subtracted field to include, and information on regional aggregation.

d) Published Results:

The results from TransCom 3, Level 1 have been published in several journal articles:

- Gurney et al. (2002) report the estimates of surface-atmosphere CO_2 fluxes from the intercomparison of the 16 transport models and model variants.
- Gurney et al. (2003) present results from that same control inversion but for individual models as well as results from a number of sensitivity tests related to the specification of prior flux information.
- Law et al. (2003) present sensitivity tests related to CO_2 data issues including network choice, time period, data selection and data uncertainty.

TransCom 3, Level 1 Output File Format

Output from the Level 1 experiment is formatted as netCDF files. This made central analysis simpler and allowed all participants a common, accessible data set for alternative analyses. The routine for writing Level 1 output to netCDF format is provided in the file <**make.output.l1.f**> at the ORNL DAAC FTP area for TransCom3, Level 1. This is an ASCII file and contains instructions and comments that should make the process of turning binary output into netCDF files.

Naming:

Each participant group submitted a number of data output files. Following the naming convention, these files provide the name of the participant's model and group (or group leader name) in place of "output" (which the netCDF writing routine produced at the beginning of the file name). For example, were Martin Heimann to submit the files containing Level I results using TM3, the file would be named, "TM3.heimann.XXX", where "XXX" is the remainder of the file name that the netCDF writing routine creates upon execution. An indication of the group or group leader is especially important for those models that are used by more than one participant.

Spatial aspects of output:

Three spatial forms were used in the Level 1 experimental output: 3D (x, y, p), 2D (x, y), and single point reporting (wind speed and tracer concentration at a single location).

1) 3D Fields:

3D fields are reported according to the longitudinal and latitudinal dimensions of each participant's model grid. In the vertical, this output was reported on the following pressure levels (in millibars) (not sigma or other model coordinate levels).

100 millibars
200 millibars
300 millibars
400 millibars
500 millibars
700 millibars
850 millibars
925 millibars
1000 millibars

Note that interpolation to pressure coordinates may have been done after time averaging the wind and tracer fields. [9] If a model does not extend to 100 mb, all of the levels listed above that are within the model domain were reported.

Any monthly mean values below the ground were reported as *missing* (see the section on "terrain masking and missing values" below).

This means that the 3D output is presented as arrays of dimension **im** x **jm** x **pm**, where **im** is the number of longitudinal grid cells in a participants model, **jm** is the number of latitudinal grid cell in a participants model, and **pm** is equal to 9 (or the maximum number of layers allowed by the model top), reflecting the pressure levels as designated above.

Following the protocol, the first grid cell of the 3D output:

- *is at the dateline* rather than at Greenwich
- *is at the south pole* rather than the north pole
- *is at 1000 mb* rather than 100 mb

Strict adherence to these conventions helped to simplify the analysis process.

---

[9] This has been done for simplicity and in recognition of the limited use of the 3D fields.

2) Maps

2D fields of the bottom two layers are reported according to the longitudinal and latitudinal dimensions of each participant's model grid. This means that the 2D field output is presented as arrays of dimension **im** x **jm**, where **im** is the number of longitudinal grid cells and **jm** the number of latitudinal grid cell in a participant's model.

As with the 3D fields, the first grid cell of the surface maps:

- *is at the dateline* rather than at Greenwich
- *is at the south pole* rather than the north pole

3) Single point reporting:

High frequency wind and tracer concentration are reported at a collection of stations. The names and coordinates of these stations are listed in the file <**statlocs.dat**> which is available for downloading at the ORNL DAAC FTP area for TransCom3, Level 1. Elevation above sea level is provided at each of these stations. Participants used whatever interpolation scheme they deemed appropriate to reflect the elevation.

Temporal aspects of output:

Two reporting time intervals are used in TransCom 3: monthly means associated with the 2D and 3D fields and a time interval determined by each participant's model timestep, associated with the single point reporting. Time is reported in UTC rather than local time.

1) 3D and 2D fields:

All 2D and 3D fields are reported as monthly means. Real, non-leap year month lengths (31, 28, 31 days, etc.) were used.

2) Single point reporting:

All single point fields are reported at a 4 hour timestep or the model timestep if it is longer than 4 hours. Single point fields are reported as instantaneous values rather than 4 hour averages.

Units:

The following units are reported:

- CO_2 concentration values as volumetric mixing ratios (parts per million by volume)

- SF_6 concentrations as volumetric mixing ratios (parts per trillion by volume)
- *u* and *v* winds in meters per second
- *w* wind in pascals/second

Terrain masking and missing values:

Explicit surface terrain masking was not required. However, all monthly mean values that reside on pressure surfaces below the ground (on pressure surfaces exceeding surface pressure) are reported as missing for that month. Missing values are reported as 1.0×10^{36} .

NOTE: monthly mean *b* values are part of the required output - if participants did not included terrain masking, an array filled with zeros was submitted to the output subroutines outlined in the protocol.

For those who included explicit surface terrain masking, the following procedure was followed:

At many locations and at many times of the year, one or more of the reporting pressure levels are below the surface of the Earth. In order to properly report 3D fields at these locations, terrain masking is employed. As shown by Boer (1982), this can be accomplished by keeping careful track of the points above ground using a terrain mask, *b*, and by carefully defining averages only over points above ground. Define *b* on pressure surfaces as

$b = 1$ for $p < p_s$
$b = 0$ for $p >/= p_s$

The representative monthly mean average of a quantity *X* is now defined by

$$\overline{X} = \frac{\overline{\beta X}}{\overline{\beta}}$$

If every timestep of a given month is below the ground, the monthly mean quantity is designated as "missing". Missing values are reported as 1.0×10^{36} .

Required output

1) Pre-subtracted tracers:

- Monthly mean 3D volumetric mixing ratio of the four pre-subtracted tracers from the last simulation year (1990 and 1995 fossil fuel, neutral biosphere, and net oceanic exchange). This represents 48 (4 CO_2 tracers x 12 months) 3D fields. ~6 MB
- Monthly mean volumetric mixing ratio maps (two lowest model layers) of the four pre-subtracted tracers from the last simulation year (1990 and 1995 fossil fuel, neutral biosphere, and net oceanic exchange). This represents 96 (4 CO_2 tracers x 12 months x 2 layers) map fields. ~2 MB

2) Terrestrial and ocean exchange basis functions:

- Monthly mean 3D volumetric mixing ratio of CO_2 for each basis function from the last simulation year for both the oceans and terrestrial basis functions. This represents 264 (22 regions x 12 months) 3D fields. ~35 MB
- Monthly mean volumetric mixing ratio maps (two lowest model layers) of CO_2 for each basis function

from the last simulation year for both the oceans and terrestrial basis functions. This represents 528 (22 regions x 12 months x 2 layers) surface map fields. ~7 MB

3) SF_6 tracers:

- Monthly mean 3D volumetric mixing ratio of SF_6 from the last simulation year for each of 11 terrestrial basis functions. This represents 132 (11 regions x 12 months) 3D fields. ~20 MB
- Monthly mean volumetric mixing ratio maps (two lowest model layers) of SF_6 from the last simulation year for each of 11 terrestrial basis functions. This represents 264 (11 regions x 12 months x 2 layers) surface map fields. ~5 MB

4) Winds:

- Monthly mean 3D fields of *u, v*, and *w* for the last simulation year. This represents 36 (3 winds x 12 months) 3D fields. ~5 MB
- Monthly mean surface map fields of *u* and *v* from the last simulation year. This represents 24 (2 winds x 12 months) surface map fields. ~0.4 MB

5) Single Point Reporting:

- High frequency station location reporting for CO_2 surface volumetric mixing ratio, *u*, and *v* from the last simulation year. These data are placed into two arrays, the first containing *u* and *v*, and the second containing the CO_2 mixing ratio for all the separate simulations. A 4 hour timestep is used for reporting this data.[10] The first array comes to (228 stations x 2190 timesteps x 2 winds) ~ 4.1 MB. The second array comes to (228 stations x 2190 timesteps x 26 CO_2 tracers[11]) ~51 MB or a total of ~55 MB.
- A text file containing the latitude, longitude, altitude, model level (or levels interpolated between) and the surface type for each site.

6) $\overline{\beta}$: (for those who computed an explicit surface terrain mask)

- Monthly mean 3D $\overline{\beta}$ values from the last simulation year. This represents 12 (1 b x 12 months) 3D fields. ~1 MB

7) Land/Sea mask

- This represents 1 surface map field. ~0.02 MB

Total ~130 MB

---

[10] If the model runs at a timestep longer than four hours, output is reported at that timestep.

[11] This represents the four pre-subtracted tracers (1990 fossil fuel, 1995 fossil fuel, neutral biosphere and net oceanic exchange) plus the 22 basis function (11 terrestrial and 11 ocean).

-

Other Relevant Information about the Study:

References:

Andres, R. J. , G. Marland, I. Fung, and E. Matthews. 1997. Geographic Patterns of Carbon Dioxide Emissions from Fossil-Fuel Burning, Hydraulic Cement Production, and Gas Flaring on a One Degree by One Degree Grid Cell Basis: 1950 to 1990. NDP-058. Carbon Dioxide Information analysis Center (CDIAC), Oak Ridge National Laboratory, Oak Ridge, TN.

Arakawa, A. and W. H. Schubert. 1974. Interaction of a cumulus cloud ensemble with the large-scale environment, Part I. J. Atmos. Sci. 31: 674–701.

Baker, D. F., R. M. Law, K. R. Gurney, P. Rayner, P. Peylin, A. S. Denning, P. Bousquet, L. Bruhwiler, Y.-H. Chen, P. Ciais, I. Y. Fung, M. Heimann, J. John, T. Maki, S. Maksyutov, K. Masarie, M. Prather, B. Pak, S. Taguchi, and Z. Zhu. 2006. TransCom 3 inversion intercomparison: Impact of transport model errors on the interannual variability of regional CO_2 fluxes, 1988–2003. Global Biogeochemical Cycles, Vol. 20, GB1002, doi:10.1029/2004GB002439.

Benoit, B. M., M. Desgagn´e, P. Pellerin, S. Pellerin, Y. Chartier, and S. Desjardins. 1997. The Canadian MC2: A semi-Lagrangian, semi-implicit wideband atmospheric model suited for finescale process studies and simulation. Mon. Wea. Rev. 125: 2382–2415.

Bousquet, P., P. Ciais, P. Peylin, M. Ramonet, and P. Monfrey. 1999a. Inverse modelling of annual atmospheric CO_2 sources and sink. Part I: method and control inversion. Journal of Geophysical Research 104: 26161-26178.

Bousquet, P., P. Ciais, P. Peylin, M. Ramonet, and P. Monfray. 1999b. Inverse modeling of annual atmospheric CO2 sources and sinks: 2. sensitivity study. J. Geophys. Res. 104: 26179–26193.

Brenkert, A. L. 1998. Carbon Dioxide Emission Estimates from Fossil-Fuel Burning, Hydraulic Cement Production, and Gas Flaring for 1995 on a One Degree Grid Cell Basis. NDP-058A. Carbon Dioxide Information analysis Center (CDIAC), Oak Ridge National Laboratory, Oak Ridge, TN.

Ciais, P., P. P. Tans, M. Trolier, J. W. C. White, and R. J. Francey. 1995. A large northern hemisphere terrestrial CO_2 sink indicated by the 13C/12C ratio of atmospheric CO_2. Science 269: 1098-1102.

D'Andrea, F. S., S. Tibaldi, M. Blackburn, G. Boer, M. Deque, M. and coauthors. 1998. Northern Hemisphere atmospheric blocking as simulated by 15 atmospheric general circulation models in the period 1979–1988. Climate Dynam. 14: 385–407.

Denning, A. S., D. A. Randall, G. J., Collatz, and P. J. Sellers. 1996. Simulations of terrestrial carbon metabolism and atmospheric CO2 in a general circulation model. Part 2: Spatial and temporal variations of atmospheric CO2. Tellus 48B: 543–567.

Denning, A. S., M. Holzer, K. R. Gurney, M. Heimann, R. M. Law, P. J. Rayner, I. Y. Fung, S.-M. Fan, S. Taguchi, P. Friedlingstein, Y. Balkanski, J. Taylor, M. Maiss, and I. Levin. 1999. Three-dimensional transport and concentration of SF6: A model intercomparison study (TransCom 2). Tellus 51B: 266-297.

Ding, P. and D. A. Randall. 1998. A cumulus parameterization with multiple cloud base levels. J. Geophys. Res. 103: 11341–11354.

Fan, S., M. Gloor, J. Mahlman, S. Pacala, J. Sarmiento, T. Takahashi, and P. Tans. 1998. A large terrestrial carbon

sink in North America implied by atmospheric and oceanic carbon dioxide data and models. Science 282: 442-446.

GLOBALVIEW-CO_2. 2000. Cooperative Atmospheric Data Integration Project–Carbon Dioxide. CD-ROM, NOAA CMDL, Boulder, CO.

Gurney, K. R., R. M. Law, A. S. Denning, P. J. Rayner, D. Baker, P. Bousquet, L. Bruhwilerk, Y-H. Chen, P. Ciais, S. Fan, I. Y. Fung, M. Gloor, M. Heimann, K. Higuchi, J. John, E. Kowalczyk, T. Maki, S. Maksyutov, P. Peylin, M. Prather, B. C. Pak, J. Sarmiento, S. Taguchi, T. Takahashi, and C-W. Yuen. 2003. TransCom 3 CO_2 inversion intercomparison: 1. Annual mean control results and sensitivity to transport and prior flux information. Tellus 55B: 555–579.

Gurney, K. R., R. M. Law, A. S. Denning, P. J. Rayner, D. Baker, P. Bousquet, L. Bruhwilerk, Y-H. Chen, P. Ciais, S. Fan, I. Y. Fung, M. Gloor, M. Heimann, K. Higuchi, J. John, E. Kowalczyk, T. Maki, S. Maksyutov, P. Peylin, M. Prather, B. C. Pak, J. Randerson, J. Sarmiento, S. Taguchi, T. Takahashi, and C-W. Yuen. 2002. Towards robust regional estimates of CO_2 sources and sinks using atmospheric transport models. Nature 415: 626-630.

Gurney, K. R., R. M. Law, A. S. Denning, P. J. Rayner, B. C. Pak, D. Baker, P. Bousquet, L. Bruhwilerk, Y-H. Chen, P. Ciais, I. Y. Fung, M. Heimann, J. John, T. Maki, S. Maksyutov, P. Peylin, M. Prather, and S. Taguchi. 2004. Transcom 3 inversion intercomparison: Model mean results for the estimation of seasonal carbon sources and sinks. Global Biogeochemical Cycles 18, GB1010, doi:10.1029/2003GB002111.

Gurney, K., R. Law, P. Rayner, and A. S. Denning. 2000. TransCom 3 Experimental Protocol. Department of Atmospheric Science, Colorado State University, USA, Paper No. 707.

Gurney, K. R., Y. H.Chen, T. Maki, S. R. Kawa, A. Andrews, and Z. Zhu 2005. Sensitivity of Atmospheric CO_2 Inversion to Potential Biases in Fossil Fuel Emissions. J. Geophys. Res. 110 (D10), 10308.

Hack, J. J. 1993. Description of the NCAR community climate model (CCM2). NCAR/TN-382, 108 pp.

Hack, J. J. 1994. Parameterization of moist convection in the National Center for Atmospheric Research community climate model (CCM2). J. Geophys. Res. 99: 5551–5568.

Hansen, J., Mki. Sato, R. Ruedy, A. Lacis, K. Asamoah and coauthors. 1997. Forcings and chaos in interannual to decadal climate change. J. Geophys. Res. 102, 25679–25720.

Hartke, G. J. and D. Rind. 1997. Improved surface and boundary layer models for the Goddard Institute for Space Studies general circulation model. J. Geophys. Res. 102: 16407–16422.

Heimann, M. 1995. The global atmospheric tracer model TM2, Technical Report, 10, Deutsches Klimarechenzentrum, Hamburg, Germany, 51 pp.

Holtslag, A. A. M. and B. A. Boville. 1993. Local versus nonlocal boundary-layer diffusion in a global climate model. J. Climate 6: 1825–1842.

Koch, D. and D. Rind. 1998. 10Be/7Be as a tracer of stratospheric transport. J. Geophys. Res. 103: 3907–3917.

Law, R. M. and P. J. Rayner. 1999. Impacts of seasonal covariance on CO_2 inversions. Global Biogeochem. Cycles 13: 845–856.

Law, R. M., Y-H. Chen, K. R. Gurney, and TransCom 3 modelers. 2003. TransCom 3 CO_2 inversion intercomparison: 2. Sensitivity of annual mean results to data choices. Tellus 55B: 580–595.

Law, R. M., P. J. Rayner, A. S. Denning, D. Erickson, M. Heimann, S. C. Piper, M. Ramonet, S. Taguchi, J. A. Taylor, C. M. Trudinger, and I. G. Watterson. 1996. Variations in modeled atmospheric transport of carbon dioxide and the consequences for CO_2 inversions Global Biogeochemical Cycles 10: 783-796.

Levy, H., J. D. Mahlman, and W. J. Moxim. 1982. Tropospheric N_2O Variability. J. Geophys. Res. 87, C4: 3061–3080.

Louis, J. F. 1979. A parameteric model of vertical eddy fluxes in the atmosphere. Boundary-Layer Meteord. 17: 187–202.

Mahlman, J. D. and W. J. Moxim. 1978. Tracer simulation using a global general circulation model: results from a midlatitude instantaneous source experiment. J. Atmos. Sci. 35: 1340–1374.

Mahlman, J. D., J. P. Pinto, and L. J. Umscheid. 1994. Transport, radiative, and dynamical effects of the Antarctic ozone hole: A GFDL "SKYHI" model experiment. J. Atmos. Sci. 51: 489–508.

Maksyutov, S. and G. Inoue. 2000. Vertical profiles of radon and CO2 simulated by the global atmospheric transport model. In: CGER report, CGER-I039-2000, CGER, NIES, Japan, v.7, 39–41.

McGregor, J. L. 1996. Semi-Lagrangian advection on conformal-cubic grids. Mon. Wea. Rev. 124: 1311–1322.

McGregor, J. L. and M. R. Dix. 2001. The CSIROConformal-Cubic Atmospheric GCM, IUTAM Symposium on Advances in Mathematical Modeling of Atmosphere and Ocean Dynamics. Kluwer Academic Publishers, Dordrecht, 197–202.

Prather, M. 1986. Numerical advection by conservation of second-order moments. J. Geophys. Res. 91: 6671–6681.

Prather, M., M. McElroy, S. Wofsy, G. Russell, and D. Rind. 1987. Chemistry of the global troposphere: fluorocarbons as tracers of air motion. J. Geophys. Res. 92: 6579–6613.

Rasch, P., N. M. Mahowald, and B. E. Eaton. 1997. Representations of transport, convection and the hydrologic cycle in chemical transport models: Implications for the modeling of short lived and soluble species. J. Geophys. Res. 102: 28127–28138.

Randall, D. A., Q. Shao, and C.-H. Moeng. 1992. A secondorder bulk boundary-layer model. J. Atmos. Sci. 49: 1903–1923.

Randall, D. A. and D.-M. Pan. 1993. Implementation of the Arakawa-Schubert parameterization with a prognostic closure, pp. 137–144. In: Emanuel, K. and D. Raymond (eds.). The Representation of Cumulus Convection in Numerical Models. American
Meteorological Society, Boston, MA.

Randerson, J. T., M. V. Thompson, T. J. Conway, I. Y. Fung, and C. B. Field. 1997. The contribution of terrestrial sources and sinks to trends in the seasonal cycle of atmospheric carbon dioxide. Global Biogeochemical Cycles, 11: 535-560.

Rayner, P. J. and R. M. Law. 1995. A comparison of modelled responses to prescribed CO_2 sources. CSIRO Division of Atmospheric Research Technical Paper No. 36.

Ritchie, H. and C. Beaudoin. 1994. Approximations and sensitivity experiments with a baroclinic semi-Lagrangian spectral model. Mon. Wea. Rev. 122: 2391–2399.

Russell, G. L. and J. A. Lerner. 1981. A new finite-differencing scheme for the tracer transport equation. J. Appl. Meteorol. 20: 1483–1498.

Schubert, S., R. Rood, and J. Pfaendtner. 1993. An assimilated dataset for Earth science applications. Bull. Am. Meteorol. Soc. 74: 2331–2342.

Strahan, S. E. and J. D. Mahlman. 1994. Evaluation of the GFDL "SKYHI" general circulation model using aircraft N2O measurements: 2. Tracer variability and diabatic meridional circulation. J. Geophys. Res. 99: 10319–10332.

Suarez, M. J., A. Arakawa, and D. A. Randall. 1983. Parameterization of the planetary boundary layer in the UCLA general circulation model: Formulation and results. Mon Wea. Rev. 111: 2224–2243.

Taguchi, S. 1996. A three-dimensional model of atmospheric CO2 transport based on analyzed winds: Model description and simulation results for TRANSCOM. J. Geophys. Res. 101: 15099–15109.

Takahashi, T., R. H. Wanninkhof , R. A. Feely, R. F. Weiss, D. W. Chipman, N. Bates, J. Olafsson, C. Sabine, and S. C. Sutherland. 1999. Net sea-air CO_2 flux over the global oceans:
An improved estimate based on the sea-air pCO_2 difference. Proceedings of the 2nd CO_2 in Oceans Symposium, Tsukuba, Japan, January 18-23, 1999.

Taylor, K. E., D. Williamson, and F. Zwiers. 2001. AMIP II Sea Surface Temperature and Sea Ice Concentration Boundary Conditions. PCMDI Report. Program for Climate Model Diagnosis and Intercomparison, Lawrence Livermore National Laboratory, University of California, Livermore, CA.

•

Tiedke, M. 1989. A comprehensive mass flux scheme for cumulus parameterization in large-scale models. Mon. Wea. Rev. 117: 1779–1800.

Point of Contact:

Kevin Robert Gurney, Ph.D., MS, MPP
Assistant Professor: Department of Earth and Atmospheric Sciences & Department of Agronomy
Associate Director: Purdue Climate Change Research Center
CIVL 2277, 550 Stadium Mall Drive
Purdue University
West Lafayette, IN 47907-2051
Phone: (765) 494-5982
Email: kevin.gurney@asu.edu

Web site: http://transcom.project.asu.edu/index.php

Revision Date: Friday, March 31, 2006